sciendo

PRODUCTION ENGINEERING ARCHIVES 2023, 29(2), 116-127

PRODUCTION ENGINEERING ARCHIVES

ISSN 2353-5156 (print)
ISSN 2353-7779 (online)

Exist since 4th quarter 2013
Available online at https://pea-journal.eu

Research of Tribological and Thermodynamic Parameters of the WC-Cu Braking System of the Experimental Modular Electric Vehicle

Daniel Varecha[1*], Jan Galik[1], Robert Kohar[2], Tomas Gajdosik[2], Igor Gajdac[2], Jozef Jenis[2]

[1] Faculty of Mechanical Engineering, Research and Service Centre, University of Zilina, Univerzitna 8215/1, 010 26 Zilina, Slovakia
[2] Faculty of Mechanical Engineering, Department of Design and Mechanical Elements, University of Zilina, Univerzitna 8215/1, 010 26 Zilina, Slovakia,
*Correspondence: daniel.varecha@fstroj.uniza.sk

Article history
Received 09.11.2022
Accepted 23.01.2023
Available online 08.05.2023

Keywords
WC-Cu coating
Friction factor
Electric vehicle
Braking system
Simulation of braking

Abstract
The authors of this manuscript present the development of a braking system with friction material base WC-Cu coating for the electric vehicle. This manuscript follows on from the original development of an AGV multi-disc braking system and an experimental investigation of the friction factor of WC-Cu coatings. In addition to developing the mechanical elements and construction of the electric vehicle, the tribological parameters of three samples of the steel substrate, the C45 with WC-Cu coating, were investigated in the tribological laboratory. A metallic coating of the WC-Cu base was applied on the C45 steel substrate using electro-spark deposition coating technology. The experiment used three samples with different percentage ratios of chemical elements in the coating structure. The tribometer working on a "Ball on Plate" principle was an investigation of the friction factor of all samples during the experiment. Subsequently, the surface of the samples was modified structure WC-Cu with laser technology. The microhardness of modified and unmodified coatings according to the Vickers methodology was investigated in the next stage. At the end of the experimental investigation, a braking simulation was created in the programming environment of the Matlab® software, considering all driving resistances. The researchers also focused on the simulation of heat conduction during braking for some considered driving modes with braking on a level and with a 20% slope roadway. The simulation of heat flow was carried out in the Matlab® programming environment using the Fourier partial differential equation for non-stationary heat conduction.

DOI: 10.30657/pea.2023.29.14

1. Introduction

The term electro – mobility refers to the movement of vehicles using electric power or, in other words, the operation of means of transport with an electric engine. Vehicles have been using energy from fossil fuels to move for more than a century. In recent years, the situation has changed (2012 – 2022), and the automotive industry is gradually bringing more vehicles into the automotive market with alternative drives. In the end, even partially hybrid vehicles belong to the field of electric mobility. About 20 years ago, the Japanese company Toyota Motor Corporation began to develop hybrid vehicles that use energy from fossil fuels to move, but also electric energy. Today, the same trend is visible in other car companies across Europe (Staniszewska et al., 2020; Rovňá et al. 2022; Klimecka-Tatar et al. 2021). Engineers of the electric vehicles left traditional friction braking systems controlled by hydraulic power to the first electric vehicles. The revolution only happened when engineers implemented a device for recuperating the vehicle's kinetic energy in electric vehicles. In this way, the engineers used energy that will lose in form heat during braking. Special drum brakes were the first devices for recuperating mechanical energy into electrical energy implemented in electric vehicles. Electric vehicles initially used an electric engine for moving only. Modern electric vehicles use to recuperate an electric engine, which turns into an electric power generator after stepping on the accelerator. Ultimately, energy recovery during braking, i.e., regaining energy when the vehicle slows down, can significantly increase the range of an electric car.

1.1. Electric vehicles and brake systems

As part of research and development at the Faculty of Mechanical Engineering was solved projects aimed at electro - mobility. The solved projects come out from the European clean and energy-saving vehicles strategy. The result of the effort was the creation of a small urban two-seat vehicle called EDISON and later EDISON II (Edison, 2013; Gajdac et al., 2019; Gajdac et al., 2014). One of the main tasks of the projects was the acquisition of new scientific information and experience in the field of development, construction and operation of electric cars and their infrastructure (Mruzek et al., 2016; Mruzek et al., 2017; Galbavy et al., 2014).

The experimental electric car EDISON II (Fig. 1) received a gold medal from the non-profit organization International Federation of Inventors' Associations (IFIA), which took place in the Czech city of Třinec in 2018 (FME, 2018).

Fig. 1. Experimental electric vehicle EDISON II (authors)

Building on previous experience, research continued towards unconventional special light electric vehicles. The idea was born for the MODULO light electric vehicle project from unconventional materials and with the electric drive (Kucera et al.,2021; Madaj et al., 2020). During the development of the experimental electric vehicle, is placed great emphasis on modular construction. Using modularity, specifically the so-called "BUS Modularity", can be changed from the basic assembly of a module with a cargo bed variation to a module with firefighting equipment. In this case, it is possible to create in a short time a vehicle for exporting wood to the vineyard, and orchards, an auxiliary vehicle for the economy, a vehicle for rescue services and many other variants (Madaj et al., 2020). We encounter examples daily, such as various vehicles, machinery, PC hardware, electrical components (switchboard components), and many others. A vehicle with an electric drive and modular construction will primarily perform special tasks in terrain with dirt roads, mud, and snow (Madaj et al., 2020). The electric vehicle is built from a kit the vehicle's drive (4WD 8000W 96V E-Car Hub) that is suitable for a total vehicle load of under 1000 kg, with maximal speed approx. 80 – 120 km/h. The MODULO experimental vehicle (Fig. 2) uses four QS273 8000W 50H V3 electric engines with permanent magnets, enabling kinetic energy recovery (qs-motor, 2022a). All electric engines' power is secure with a 96V battery. (qs-motor, 2022b).

Fig. 2. Experimental electric vehicle MODULO CAD model (authors)

The automotive industry is on the verge of a revolution, as it is gradually moving from a hydraulic system to an electric one, which will be in line with future vehicles (Brembo, 2022). Brembo is very dedicated to brake-by-wire, not only for road person vehicles but also for racing cars (Brembo, 2022). Development trends indicate that mechanical control systems based on hydraulic energy are increasingly being omitted in modern electric cars and replaced by energy recovery systems (Tomasikova et al., 2017). These technological changes are being incoming at the beginning of the coming fourth industrial revolution, which is also called in some publications the digital revolution. Ultimately, Industry 4.0 is considered a new industrial stage that can help companies achieve higher industrial performance (Narula et al., 2021). New technologies enable an ever-higher level of production efficiency. They also have the potential to influence social and environmentally sustainable development (Bai et al., 2020) dramatically.

There are different brake force control systems in practice, but not all are usable in this project. For this reason, the experimental electric vehicle provided a brake system with an electromechanical brake force control system. The electromechanical control mechanism of the brake force is designed according to the rules for the safety of electrical and electronic vehicle systems (ISO 26262) (Synopsys, 2022). The brake system primarily ensures vehicle braking in critical situations (assistance during braking by recuperation) and, if necessary, serves as a "bypass" in recuperation failure. For example, Volkswagen ID.3 vehicles use brake energy recovery using highly modern drum brakes on the rear axle (Volkswagen, 2022). The vehicle uses traditional disc brakes at the other end (Volkswagen, 2022).

When braking a vehicle with a heavy load, a large amount of inertial energy is generated, which still pushes the vehicle forward during braking and should be remembered (Varecha et al., 2019a; Varecha et al., 2019b). However, the experimental electric vehicle's engine can work as a generator during deceleration, simultaneously charging the battery and, at the same time, developing a regenerative braking torque on the axle (Qiu et al., 2018). In critical situations, braking with only the electric engine (recuperation) is ineffective due to the increased braking distance at high speed (80 km/h). This fact is one of the several reasons why the developers of the electric vehicle also equipped the vehicle with a braking system. Control of the braking force will not be ensured conventionally secured (hydraulic and pneumatic control system) but by

a mechatronic system (Tropp et al., 2017a; Tropp et al., 2017b). Paradoxically, the hydraulic brake force control system brings greater efficiency. However, environmental pollution may occur if the pressure oil distribution system is damaged. Finally, the production of compressed oil, in the case of compressed air, is an energy-intensive process. Saving and efficient use of energy is currently a growing trend in Europe. The electromechanical control brake system consumes significantly less energy for its operation. Ultimately, the energy savings that occur during vehicle operation have a direct positive effect on the vehicle's range, and, ultimately, the environment in this way is saving. The electromechanical brake force control system is set in motion by electricity from the vehicle's battery. The brake system is placed on the output shaft of each electric engine (Fig. 3a) and bolted. The illustration from the laboratory shows a realistic view of the location of the electric engine in the space of the sheet metal disc with the tire (Fig. 3b). The vehicle has shoes on with high-quality tires designed for rocky and hard terrain.

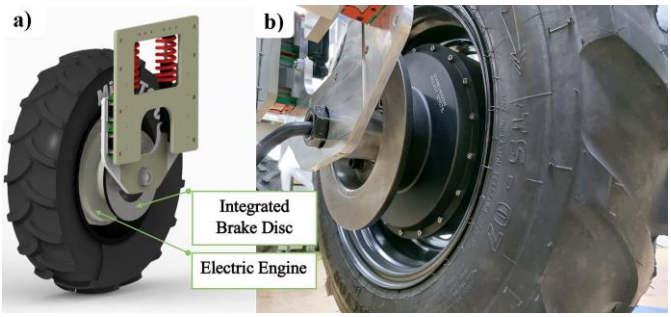

Fig. 3. Parametric 3D model of part of the axle and braking system of an electric vehicle (a), the experimental electric vehicle in the laboratory (b) (authors)

The brake system of the experimental vehicle consists of a cast-iron disk and brake pads with a WC – Cu coating. Researchers have previously (2021) worked on a multi-disc braking system for automated guided vehicles (AGVs) with WC – Cu coated friction discs. Porsche also tested the brake system based on Porsche Surface Coated Brake technology on the Cayenne model. After thousands of kilometres, the brakes of the Porsche Cayenne test vehicles were still clean (Porsche, 2022). In parallel with the experimental investigation of the friction factor run development of some mechanical parts of the vehicle. The development partial results were subsequently published (Madaj et al., 2021) in the local journal in the Slovak language.

2. Experimental investigation of the friction factor of the coated substrate of C45 steel

Researchers from the Faculty of Mechanical Engineering have many years of experience in the experimental investigation of tribological and corrosion properties of steels (Liptakova et al., 2017). The area of investigation is also extended to surface topography by the Alicona device (Jambor et al., 2020). Also, researchers are engaged in analysing the roughness profile on curved surfaces (Drbúl et al, 2018). The current experimental investigation of tribological parameters smoothly follows from the original investigation of WC – Cu coatings of 2020, and 2021 years, only with a modified percentage ratio of WC – Cu chemical elements in the structure of the coating and a new setting of the testing time interval. The publication (Varecha et al., 2021) published in the internationally recognised. The authors of the manuscript (Varecha et al., 2021) state that the correct WC – Cu ratio forms the basis for the proper functioning of the brake system. A WC – Cu coating was applied to the surface of all samples using electro – spark deposition (ESD) technology (Radek et al., 2018; Konstanty et al., 2015; Radek et al., 2010; Radek et al., 2020) (Fig. 4). Consequently, in the tribological laboratory conducted the experimental investigation of the friction factor of three samples of the substrate steel C45 with different WC – Cu ratios in the coating. Subsequently, all samples' WC – Cu coating structure with laser technology was modified. The laser technology removed the rough spots (peaks), which obtained a more even and smooth surface (Fig. 5).

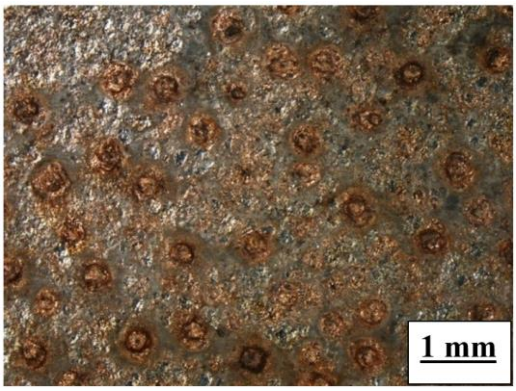

Fig. 4. Surface structure of unmodified WC – Cu coating (Varecha et al., 2020)

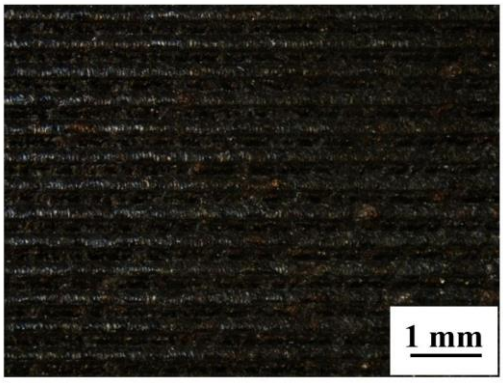

Fig. 5. Surface structure of WC – Cu coating after Laser Remelting (Varecha et al., 2021)

The exact percentage ratio of WC – Cu hard materials in the structure of the coating and the measured hardness values according to the Vickers methodology listed for each sample in the table below (Tab. 1). This type of hardness test was performed according to the national standard EN ISO 6507 – 1. After laser modification, the ESD coatings obtained a visibly more uniform and smoother surface. Still, on the other hand, the additional laser treatment slightly reduced the hardness of the treated coating. The authors of publications (Varecha et al., 2021; Kraus, 1980) also describe this claim.

Table 1. List of WC–Cu percentage ratio and micro hardness test of all samples (authors)

Samples	Coating	WC	Cu	HV 0.5 before laser modification	HV 0.5 after laser modification
ESD-No.01-2022	WC25 – Cu75	25 [%]	75 [%]	631 [-]	590 [-]
ESD-No.02-2022	WC50 – Cu50	50 [%]	50 [%]	675 [-]	631 [-]
ESD-No.03-2022	WC75 – Cu25	75 [%]	25 [%]	651 [-]	630 [-]

The laser-modified (remelting) WC – Cu coatings were subjected to a tribological test to investigate the friction factor for all three samples. The experimental investigation of friction factor went on a tribometer (Fig. 6) which worked on the principle of a moving steel ball on the sample's surface with a sliding distance of 50 mm. The weight acting on the steel ball created the normal force which acts on the tribological pair during the experiment. The tribological test was carried out in the laboratory under atmospheric conditions without lubrication. The speed of the moving steel ball on the surface sample had a sinusoidal curve in the v = 0 to 20 mm/s.

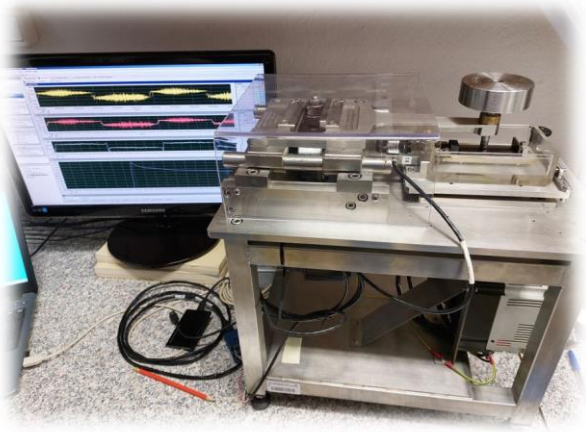

Fig. 6. Tribometer in laboratory (authors)

The laser-modified WC-Cu coating has a uniform surface structure but slightly lower micro-hardness than the unmodified WC-Cu coating. After modifying the surface with a laser, the micro-hardness decreased from 3.2 to 6.5%, but these values are acceptable, and the substrate of steel C45 coated in this way can use in the brake system. The experimental investigation of friction factors is discrete into two stages. The first stage lasted 1,000 seconds (16.67 minutes) and done into two stress phases. The first phase of the experimental investigation is samples loaded with a value of 1 N. It can see from the diagram that a larger ratio of tungsten carbide (WC) in the structure of the coating causes an irregular, oscillating curve (Fig. 7).

The coating structure with a higher proportion of copper (75%) shows a highest friction factor of all three samples that load with 1 N. However, the higher concentration of copper (Cu) in the coating structure causes soft places, as seen in the following diagrams (Fig. 8 – 9). The high tungsten carbide (WC) content reduces the friction factor, which manifests in the irregular and rough curve (Fig. 7).

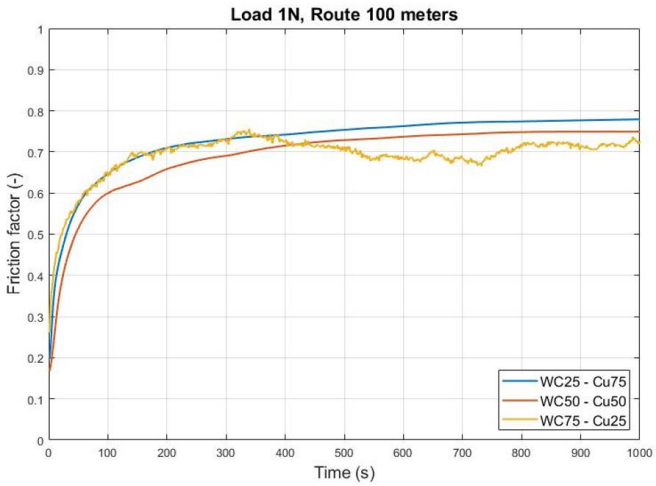

Fig. 7. The tribological pair loaded with 1 N, distance 100 meters (authors)

In the second phase of the experimental investigation, all samples loaded are with a force of 5 N. As can be seen from the diagram (Fig. 8), a higher load revealed soft spots in the structure of the WC25 – Cu75 coating. Around the middle of the test (500 seconds), there was a decrease in the friction factor, which ultimately caused a fluctuating and rough course of the curve of friction factor. The little, bigger load force (5 N) during the test revealed that the coating structure with a higher proportion of tungsten carbide (WC) has a higher micro-hardness. The rough and fluctuating course of the friction factor of the sample WC75 – Cu25 by the greater microhardness is caused (Fig. 8). The uniformly distributed ratio of WC – Cu hard materials in the structure of the coating manifested itself in a clear and smooth course with an almost constant friction factor (Fig. 8). A similar friction factor result can also be seen at the sample loaded with 1 N (Fig. 7). In the last stage of the experimental investigation, the last three WC – Cu coatings are subject to friction factor investigation in the longest time interval of 5000 seconds (83.33 minutes).

In the long-term phase of the experimental investigation of the friction factor (Fig. 9) is observed similar course of the friction factor as in the first short stage. As observed in the previous diagrams, a larger proportion of copper in the WC - Cu coating structure increases the friction factor. However, the coating is softer and prone to more wear and tear. The result is an oscillating waveform in the shape of a ridge. Conversely, a higher ratio of tungsten carbide causes a coarse and unyielding structure with a low or decreasing friction factor (Fig. 9).

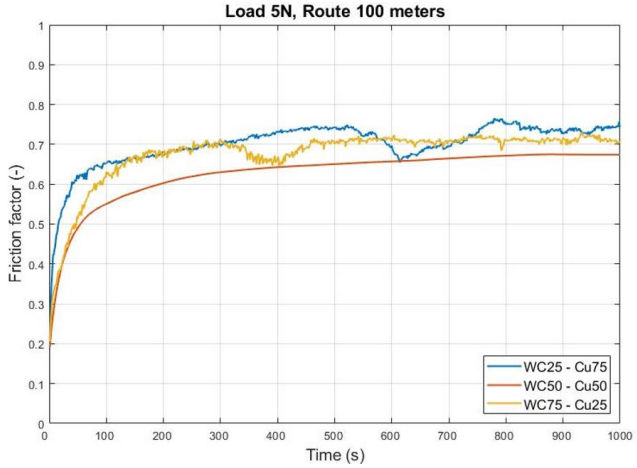

Fig. 8. The tribological pair loaded with 5 N, distance 100 meters (authors)

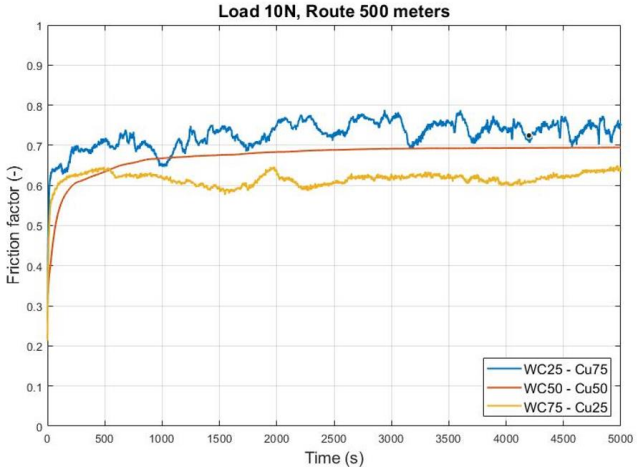

Fig. 9. The tribological pair loaded with 10 N, distance 500 meters (authors)

The last diagram in the sequence shows the friction factor's dependence at the experiment's time (Fig. 10) for three WC50 – Cu50 coating samples with a uniformly distributed ratio of chemical elements in the coating structure.

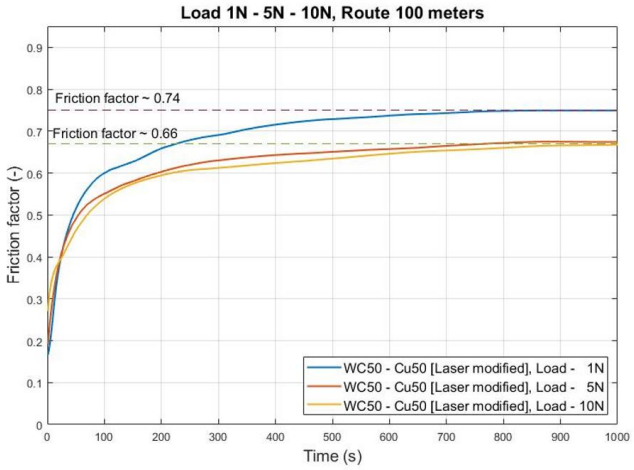

Fig. 10. Results of the tribological pair, size load of 1 until 10 N (authors)

The three curves present the different courses of the friction factor obtained during the tribological experiment. Loaded every sample with a different normal force corresponding to 1 N, 5 N to 10 N. Turing the evaluation of three coated WC – Cu modified samples, a decrease in the value of the friction factor is visible as the force increases. Between the load of 1 N and 10 N was observed, a decrease in the friction factor of 10.8%. It is also necessary to point out that the value of the friction factor was almost identical with a load of 5 N to 10 N. Researchers assume that by increasing the load (normal force), the value of the friction factor should not fall below 0.6 (Fig. 10).

The friction factor (f) results describe table below (Tab. 2). The friction factor's arithmetic means were calculated (Eq. 1) from the measured tribological data set of three samples with laser-modified WC – Cu coating. Loading every mentioned sample's normal force was during the tribological test different.

$$\bar{x} = \frac{1}{n} \times \sum_{i=1}^{n} x_i = \frac{x_1 + x_2 + x_3 \ldots + x_n}{n}; [-] \quad (1)$$

Table 2. Arithmetic mean of friction factor for three loads of normal force (authors)

Samples	Load 1 [N]	Load 5 [N]	Load 10 [N]
ESD-No.01-2022	0,77 [-]	0,72 [-]	0,70 [-]
ESD-No.02-2022	0,74 [-]	0,67 [-]	0,66 [-]
ESD-No.03-2022	0,70 [-]	0,71 [-]	0,63 [-]

3. Simulation of braking electric vehicle MODULO

Researchers determined the basic design and operating parameters of the MODULO experimental electric vehicle at the beginning of its development. The electric vehicle is designed for operation in different areas of the region. Therefore, it will drive in three modes limited by the maximum speed (Tab. 3).

Table 3. Basic structural and operational parametric of electric vehicle (authors)

Weight of electric vehicle (Including driver & cargo)	Drive Mode			Maximal Rise / Slope
700 kg	TRIP 80 km/h	RACE 50 km/h	MUD 30 km/h	0 – 20%

It is known from practice that it is impossible to drive at high speed in every terrain. Researchers set speed limits, which are listed table below (Tab. 4). The electric vehicle MODULO uses four electric engines to move, which can provide the vehicle with a speed of up to 120 km/h. However, for design, operational and safety reasons, the vehicle's speed limit in the "TRIP" driving mode was set at a maximum speed of 80 km/h and only for driving on a quality asphalt road. The "RACE" driving mode is speed lowered to 50 km/h due to the terrain in which the vehicle moves. The last "MUD" driving mode is typical of the speed limit set to 30 km/h. Drive on the "TRIP" driving mode is recommended on a quality asphalt roadway. The vehicle can drive in "RACE" mode, in addition to a high-

quality asphalt roadway, on an unpaved dry dirt road and grassy terrain. In the last "MUD" driving mode, the vehicle can drive in light mud or on loose snow. The "MUD" driving mode can also be allowed for driving on the roadways /terrains mentioned above.

Table 4. Speed limits of driving modes for the considered area of the region (authors)

Type of terrain and coefficient of rolling resistance roadway	Speed of electric vehicle		
	30 km/h	50 km/h	80 km/h
Asphalt roadway ($R_{rl} = 0.01$)	☑	☑	☑
Dry dirt road ($R_{rl} = 0.04$)	☑	☑	N/A
Grassy terrain ($R_{rl} = 0.08$)	☑	☑	N/A
Loose snow/Mud ($R_{rl} = 0.2$)	☑	N/A	N/A

The electric car is driven primarily by electric engines, which are used for moving the vehicle and secondarily for braking by recuperating kinetic energy into electrical energy. Recuperation ensures the slowing down or complete braking of the electric vehicle. During the development of the electric vehicle, researchers considered various brake systems. Finally, was chose a brake system with a brake disc. The brake system comprises a cast iron disc and two steel brake pads within WC – Cu coating. The cast iron disc's structural and thermal parameters state in the table below (Tab. 5).

Table 5. Structural and thermal parameters of cast iron disc (authors)

Description	Young's Modulus	Poisson's Ratio	Isotropic Thermal Conductivity	Specific Heat Constant Pressure
Value	1.1e+11 [Pa]	0.28 [MPa]	52 [W/m×°C]	447 [J/kg×°C]

The braking simulation was created in Matlab® computer software using Newton's motion equations (Eqs. 2 - 4) with the implementation of all driving resistances (Eqs. 5 - 8) that affect the MODULO electric vehicle while driving.

$$v(t) = -\frac{F_{Brake}}{m} \times t + v_0\,;\ \left[\frac{m}{s}\right] \tag{2}$$

$$s(t) = -\frac{F_{Brake}}{2 \times m} \times t^2 + v_0 \times t + s_0\,;[m] \tag{3}$$

$$a = -\frac{F_{Brake}}{m};\ \left[\frac{m}{s^2}\right] \tag{4}$$

where: v(t) is final velocity in time [m/s], F_t is maximum tractive effort [N], F_{Brake} is total brake force [N]. m is vehicle mass, t is time [s], v_0 is initial velocity of vehicle [m/s], s(t) is final braking route [m], s_0 is initial location [m], a is deceleration [m/s^2].

The first resistance is the rolling resistance (Eq. 5). This resistance is directly dependent on the weight of the MODULO electric vehicle. Also, the tires affect the value of the rolling resistance, mainly the contact with the roadway. It should also note that the value of the rolling resistance changes slightly depending on the vehicle's speed.

$$R_{rl} = W \times C_{rr} \times cos(\theta)\ ;\ \ [N] \tag{5}$$

where: W is vehicle weight [kg], C_{rr} is coefficient of rolling resistance roadway [-] a θ is slope/grade roadway [°]. Aerodynamic resistance is the second resistance that acts on an electric vehicle during driving (Eq. 6).

$$R_a = 0.5 \times \rho_{air} \times C_d \times A \times V^2; [N] \tag{6}$$

where: ρ_{air} is air destiny [kg/m3], C_d is coefficient of drag [-], A is projected frontal area [m^2], V is speed of the vehicle (headwind velocity) [m/s]. The vehicle during driving overcomes a maximum rise/slope from 0 to 20% (Eq. 7).

$$R_g = W \times sin(\theta)\,;[N] \tag{7}$$

where: R_g is grade resistance, θ is slope roadway [°]. Ultimately, the resulting braking force is the sum of all the mentioned resistances, including the force induced by the braking system (Eq. 8). For driving at a constant speed, the acceleration resistance R_I will be zero.

$$F_t = F_{Brake} + R_{rl} + R_a + R_g + R_I\ ;\ \ [N] \tag{8}$$

According to the specified operating parameters, calculated the results of driving resistances for individual driving modes were in the Matlab® programming software (Tab. 6).

Table 6. Results of driving resistance acting on the vehicle during driving (authors)

Speed of vehicle [km/h]	Coefficient of Road Rolling resistance C_{rr} [-]				Aerodynamic Resistance R_a [N]	Grade Resistance R_g [N]		
	0.01	0.04	0.08	0.2		0 [%]	10 [%]	20 [%]
	Rolling resistance R_{rl} [N]							
30					69.8			
50	68.7	274.7	549.4	1 373.4	193.9	0	-1 421.5	-2 005.2
80					496.5			

Driving resistances that act against a moving electric vehicle consume part of the energy of the electric engine and affect the vehicle's final braking distance. The following table (Tab.7) presents the braking distance results for a vehicle braked on a level roadway.

The braking distance extends when the vehicle is braking down the slope. In this case, the electric vehicle braked on the roadway with a 10% slope. Results of the braking simulation have listed in the table below (Tab.8).

Table 7. The braking distance of the electric vehicle when braking on a level roadway (authors)

Road slope 0% - Driving on the flat and total braking route [m]			
Speed of vehicle	30 km/h	50 km/h	80 km/h
Asphalt roadway	4.71 m	13.06 m	32.35 m
Dry dirt road	4.53 m	12.56 m	N/A
Grassy terrain	4.30 m	N/A	N/A
Loose snow / Mud	3.76 m	N/A	N/A

Table 8. The braking distance of the electric vehicle when driving on roadway with a 10% slope (authors)

Road slope 10% Descending of the road and total braking route [m]			
Speed of vehicle	30 *km/h*	50 *km/h*	80 *km/h*
Asphalt roadway	6.53 *m*	18.00 *m*	44.10 *m*
Dry dirt road	6.10 *m*	17.07 *m*	N/A
Grassy terrain	5.78 *m*	N/A	N/A
Loose snow / Mud	4.82 *m*	N/A	N/A

The last table (Tab. 9) presents the results of the braking distance for a vehicle that braked on the roadway with a 20% slope. The results of the braking simulation show, that the speed limits for the electric vehicle set by the developers are necessary. The results of the braking simulation are also presented graphically in the next chapter.

Table 9. The braking distance of the electric vehicle when driving on roadway with a 20% slope (authors)

Road slope 20% Descending of the road and total braking route [m]			
Speed of vehicle	30 *km/h*	50 *km/h*	80 *km/h*
Asphalt roadway	7.76 *m*	21.30 *m*	51.89 *m*
Dry dirt road	7.28 *m*	20.00 *m*	N/A
Grassy terrain	6.72 *m*	N/A	N/A
Loose snow / Mud	5.46 *m*	N/A	N/A

4. Simulation of Braking and Heat Flow of the Braking System During Braking

The speed of the MODULO electric vehicle is limited to three driving modes. Due to very much numerical data was prepared in the programming environment of the software MATLAB, only the braking simulation of the second (RACE, V_{max} = 50 km/h) and third driving modes (TRIP, V_{max} = 80 km/h). At the start of the braking simulation, driving mode "RACE" is divided into two stages. The first stage of the simulation is to investigate the braking route of the vehicle on a flat dirt road with a speed of 50 km/h, and in the second stage braking route of the vehicle on a dirt road with 20% slope. The braking distance of the electric vehicle on a flat dirt road in this driving mode is 12.56 m (Fig.11). The braking distance of a vehicle driving on a dirt road with a slope of 20% increased to 20.0 m (Fig.12), which is 58.7% increase compared to braking on a flat dirt road. In other words, a vehicle driving on a dirt road with a 20% slope during braking will cover 7.44 m more distance with a longer braking time of 1.1 seconds.

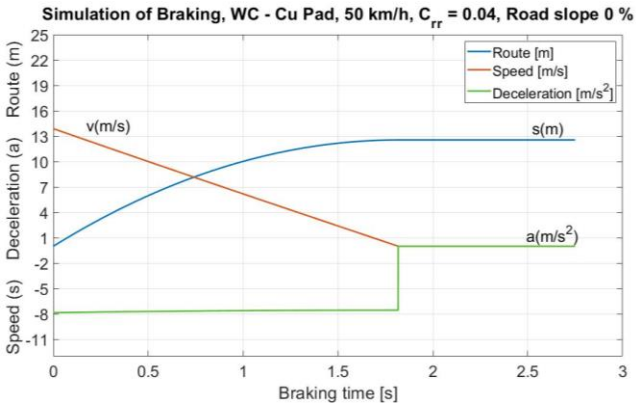

Fig. 11. The simulation of vehicle braking from a speed of 50 km/h on a flat dirt road (authors)

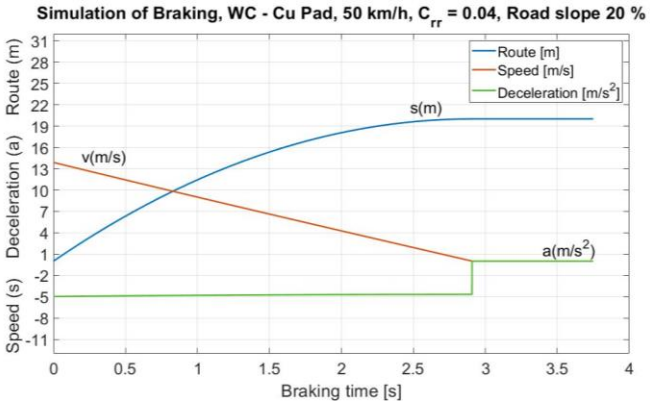

Fig. 12. The simulation of vehicle braking from a speed of 50 Km/h during a 20% slope of a dirt road (authors)

In the programming environment of the Matlab software was prepared simulation of the heat flow in the braking system during the one-time braking of the electric vehicle with think two driving modes. The mechanical energy during braking is changed into thermal energy (Kraus, 1980). The computational software Matlab® uses the Fourier partial differential equation for non-stationary heat conduction for temperature profile calculation (Eq. 9, Appendix A) (Kruas, 1980; Siedlecka, 2019; Spałek, 2018). The issue of the Fourier theory is well-described authors of the publication (Wolf, 1979).

During the simulation of het flow in the brake system of the electric vehicle with a driving speed of 50 km/h on a flat dirt road and own weighing 700 kg produced the temperature on the surface of the brake disc to almost 60 °C during braking (Fig. 13). From the diagram, you can see a large increase in temperature in a short time in the area of contact between the brake disc and the brake pad with a WC - CU coating. A different result of the temperature profile is visible when braking an electric vehicle on the same terrain with only a 20% slope of dirt road. The braking distance has extended during braking on a dirt road with 20% slope, resulting in a long time of act frictional between the brake pad and brake disc. The simulation found that the maximum temperature during braking in the contact between the brake disk and the brake plate is 50°C (Fig. 14). However, the temperature in the brake system increased gradually during braking, as illustrated in the diagram

(Fig. 14), which has a shallower temperature profile. The brake disc absorbed more heat in this driving mode during braking.

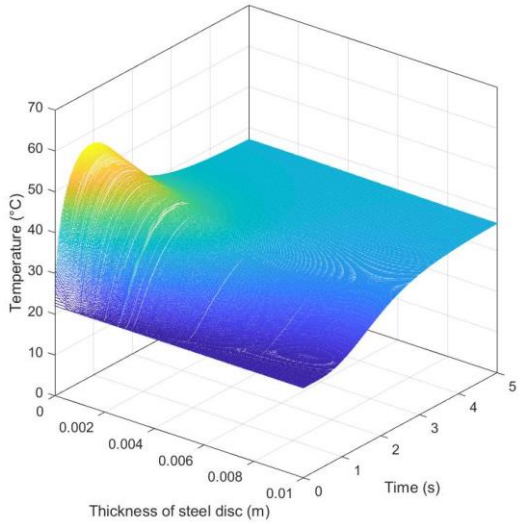

Fig. 13. Temperature profile during braking from 50 km/h speed on a flat dirt road (authors)

The electric vehicle's driving in the third driving mode was set at a speed of 80 km/h and reserved only for high-quality asphalt roadways. The designers carefully considered this decision also, given the strict regulations and laws on road traffic in the Slovak Republic, including the regulations of the European Union. It is known from practice that the braking distance increases with increasing speed. In this case, too, the braking simulation showed that a vehicle driving on a flat asphalt roadway at a speed of 80 km/h and with an own weight of 700 kg increased the resulting braking distance to 32.35 m (Fig. 15). The electric vehicle braking on an asphalt roadway with a slope of 20% has the braking distance extended by 19.54 m to a value of 51.89 m (Fig. 16).

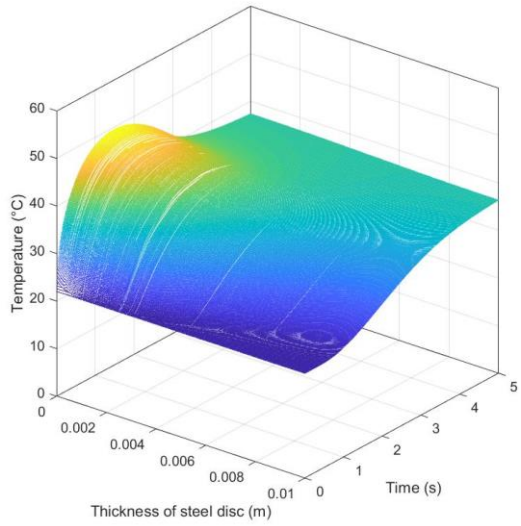

Fig. 14. Temperature profile during braking from a speed of 50 km/h during a 20% slope of a dirt road (authors)

In this case, it is a 60.4% increase in braking distance compared to braking on an ideally flat road without descent. In this case, the braking time increased by 1.8 seconds, representing a 61.8% increase compared to the braking time of the vehicle on the level roadway. Ultimately, for the designer of brake systems, the vehicle's braking distance is an authoritative figure, according to which it is possible to evaluate the overall performance and efficiency of the brake system. When the electric vehicle braked from a speed of 80 km/h manifested greater kinetic energy in a significantly longer braking distance. The temperature in the contact between the brake pad and the brake disc increased significantly, and the brake disc absorbed greater heat. Also, the braking system produces more heat than in the driving mode of "RACE" with a speed of 50 km/h.

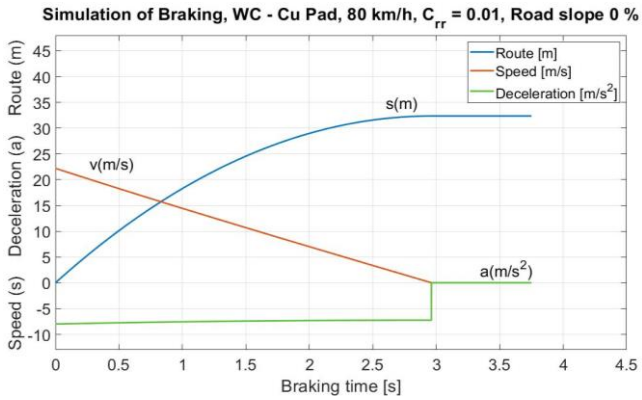

Fig. 15. The simulation of vehicle braking from a speed of 80 km/h on a flat roadway (authors)

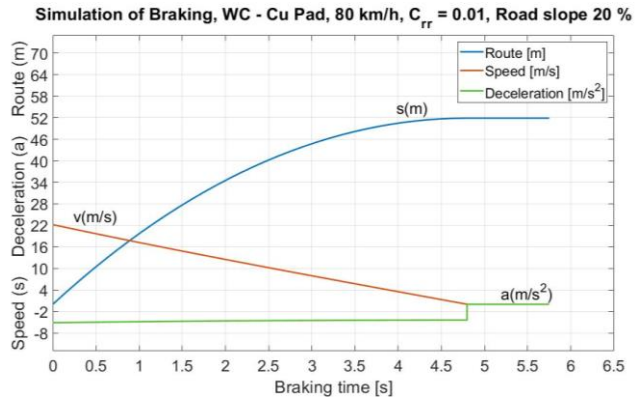

Fig. 16. The simulation of vehicle braking from a speed of 80 km/h on a flat roadway (authors)

The brake system absorbed a greater quantity of heat during braking of the "TRIP" driving mode. During the braking of the vehicle in the "TRIP" mode from a speed of 80 km/h on a flat asphalt roadway, a temperature of over 300 °C arose in the contact between the brake disc and the brake pad with WC - Cu coating (Fig. 17). From the diagram, you can see a sharp rising wave of the temperature profile, which after braking starts to drop down quickly.

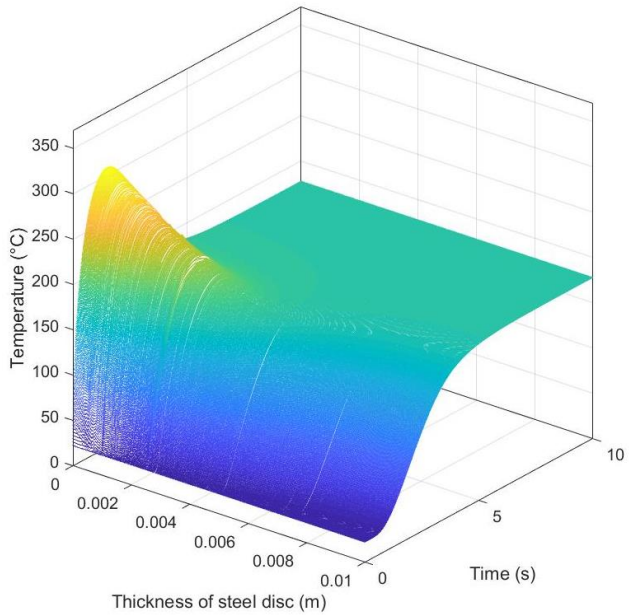

Fig. 17. Temperature profile during braking from 80 km/h speed on a flat asphalt roadway (authors)

The result of the simulation of heat flow in the braking system of an electric braking vehicle driven with a speed of 80 km/h on an asphalt roadway with a 20% slope indicated a different result of a temperature profile (Fig. 18).

The braking time is extended by 1.8 seconds in this case, and this caused the brake disc to absorb heat over a relatively long time. The temperature at the contact between the brake disc and the brake pad is relatively lower (~ 250 °C) as the first case (Fig. 17). However, the diagram shows that the brake disc absorbed the significantly biggest amount of heat into the brake disc.

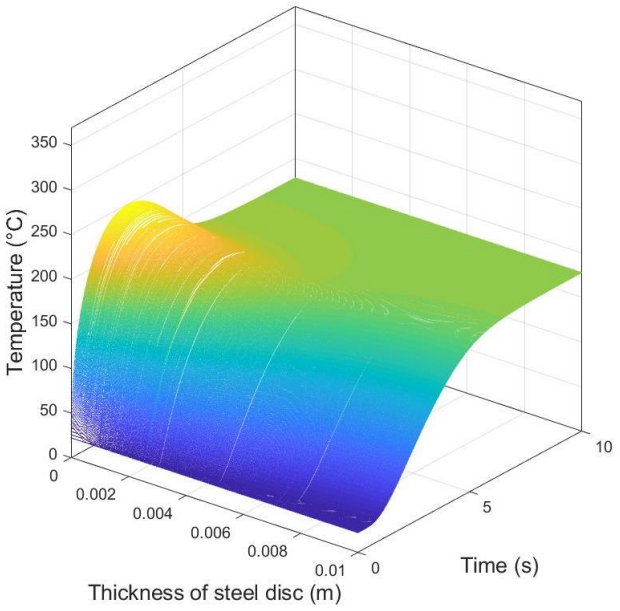

Fig. 18. Temperature profile during braking from a speed of 80 km/h during a 20% slope of a dirt roadway (authors)

5. Conclusion and Discussion

Developing a modular electric vehicle represents a set of complex processes and research activities necessary for developing electric vehicles. One of the important parts of any vehicle is the functional and effective brake system. In the 21st century, several types of brake system constructions are available. A Very important chapter in the area of brake systems represents brake materials. From practice are mainly known as sintered brake materials based on metal powder. Also, are used organic and metal-ceramic friction materials. The braking system of the car company Porsche, which developed a brake system based on the Porsche Surface Coated Brake (PSCB) technology, inspired mechanical engineering researchers of multi-brake system with WC – Cu coating already in the past. In the tribological laboratory (2020 – 2021) experiment with WC – Cu coatings was launched for this reason. The Faculty of Mechanical Engineering researchers were looking for the correct percentage ratio of chemical elements WC – Cu, which would have a friction factor with a linear course and with resistance to wear and excellent long service life. The multi-brake of automated guided vehicles (AGVs) system was developed based on the experimental investigation of the friction factor. The issues of producing new materials based on WC and Cu and searching for their applications are still current topics for many researchers (Dias et al., 2018; Tejado et al., 2018). Copper is a corrosion-resistant material with high thermal conductivity. In addition, as a coating material, it reduces residual (tensile) deformations and improves adhesion (Radek et al., 2009; Zhao et al., 2004). The research has nowadays extended to experimental investigation of the friction factor of brake pads with WC – Cu coating for the braking system of the modular electric vehicle. Subsequently, a new experimental investigation of the friction factor of WC – Cu coatings took place in the tribological laboratory by applying new boundary conditions. The change occurred in the percentage composition of chemical elements WC – Cu in the coating structure and the experimental investigation stage, divided into two distances of 100 and 500 meters. From a long-term experimental investigation (500 meters), it is clear that the WC50 – Cu50 combination has the most stable course of the friction factor. This fact is best seen in Figure 8, while one more very important data is visible, namely, the total value of the friction factor. During a load of 1 N, the value of the friction factor is the largest (f ~ 0.74), but with subsequent loads of 5 and 10 N, the friction factor slightly decreased and stabilized at the value of f ~ 0.66. The researchers conducted the experimental investigation of the friction factor several times in the tribology laboratory, and the results were always in the range from f ~ 0.6 to 0.78. It is also necessary to point out that the stated values of the friction factor apply only to the WC50 – Cu50 combination. It should note that current experimental research of friction factor WC – Cu coating confirmed the results also measured in the tribological laboratory during the AGV lamellar brake system project from 2020 to 2021. It is supposed that the value of the friction factor should not fall below the value of 0.6 by increasing the load (Normal Force). The statement that a value of friction factor does not fall below

0.6 will confirm or refute by experimental testing in terrain only. Of course, the developers are also interested in the service life brake system. This parameter is reviewable only at the vehicle in a test operation.

When researching and developing new braking systems for electric cars, it is necessary to focus on computer modelling, braking simulation and testing new brake systems before production or possibly subsequent operation. For objective and safety reasons, the developers of the electric vehicle specified three driving modes, which define the maximal speed limit of the vehicle. The choice of driving modes was the right step from the side of the researchers because the vehicle is ready to drive off-road with a 20% slope roadway. The simulation of the braking system was done in the programming environment of the Matlab® software using Newton's equations of motion. Braking simulation found that when braking on a dry dirt road with a 20% slope, the braking distance increases significantly at speeds above 50 km/h.

In the last stage of the development of the brake system, the developers also focused on the simulation of the heat flow in the brake system with a WC – Cu friction pad. The heat flow simulation was created in a programming environment MATLAB using the Fourier partial differential equation for non-stationary heat conduction. The results of the heat flow simulation present the progress of the temperature profile that arises in the contact between the WC – Cu brake pad and the cast iron disc during a single depression of the brake pedal. During the heat flow simulation, an extreme case occurred when braking the electric vehicle in "TRIP" driving mode on a 20% slope roadway. Even when braking on a flat roadway. In this case, the temperature rose to 250 to 300 °C at the friction contact between the brake pad and disc. However, it should note that the monitored temperature of 300 °C is standard during braking under the mentioned operating conditions and is the same on all four brake discs' surfaces.

The developers plan to verify the results from the braking simulation in individual driving modes after the final assembly of the electric vehicle verify in practice. Researchers will prepare the experimental testing shortly in section terrain. The field research study will also focus on the heat generated during braking. Developers are also interested in the temperature profile after repeated braking of the braking system.

The MODULO project is a current topic due to its focus and insight into the issue of mobility in various terrains of the region with the use of the electric drive. The emphasis on the research part in the field of braking systems is clear due to the safety of the electric vehicle. Outputs from ongoing research activities provide the basis for further development, simulations, experiments, testing and prototype electric vehicle implementation.

In conclusion, the authors of the manuscript would like to emphasize that the comprehensive implementation of research activities in the use of non-conventional vehicle drives enables cooperation in the development activities of organizations forming part of the e-mobility platform and cooperation in the creation of legislative changes.

Acknowledgements

This article was funded by the University of Žilina project 313011ASY4—"Strategic implementation of additive technologies to strengthen the intervention capacities of emergencies caused by the COVID – 19 pandemic and the Slovak Research and Development Agency under contract No. APVV-18-0457.

Reference

Bai, Ch., Dallasega, P., Orzes, G., Sarkis, J., 2020. Industry 4.0 technologies assessment: A sustainability perspective, International Journal of Production Economics. 229, 107776, DOI: 10.1016/j.ijpe.2020.107776

Brembo, 2019, A Leap Into The Future With Brembo Brakes: Changing The Way You Drive With Benefits For Drivers And For The Environment. available at: https://www.brembo.com/en/company/news/future-brake (accessed 5 October 2022)

Dias, M., Guerreiro, F., Tejado, E., Correia, J., Mardolcar, U., Coelho, M., Palacios, T., Pastor, J., Carvalho, P., Alves, E., 2018. WC-Cu thermal barriers for fusion applications, Surface and Coatings Technology. 355, 222-226, DOI: 10.1016/j.surfcoat.2018.02.086

Drbul, M., Martikan, P., Broncek, J., Litvaj, I., Svobodová, J., 2018. Analysis of roughness profile on curved surfaces. Innovative Technologies in Engineering Production (ITEP'18), Bojnice, Slovakia, 01024.

Edison (2013), "Project of electric vehicle", available at: http://www.edison.uniza.sk. (accessed 5 October 2022)

Gajdac, I., Gajdosik, T., Steininger, J., 2017. The Energy Assist for the Electric Car Edison. 12th international scientific conference of young scientists on sustainable, modern and safe transport, High Tatras, Slovakia, 251-264.

Gajdac, I., Kamas, P., 2018. Computing and Design of Electric Vehicles, 59th International Conference of Machine Design (ICMD 2018). Zilina, Slovakia, 105-111.

Galbavy, M., Pitonak, J., Kucera, L., 2014. Powershift Differential Transmission with Three Flows of Power for Hybrid Vehicles. 54th International Conference of Machine Design Departments, Liberec, Czech Republic, 27-33.

Jambor, M., Kajanek, D., Fintova, S., Broncek, J., Hadzima, B., Guagliano, M., Bagherifard, S., 2020. Directing Surface Functions by Inducing Ordered and Irregular Morphologies at Single and Two-Tiered Length Scales. Advanced Engineering Materials, 23 (2), 1-15, DOI: 10.1002/adem.202001057

Klimecka-Tatar, D., Ingaldi, M., Obrecht, M., 2021. Sustainable Development in Logistic - A Strategy for Management in Terms of Green Transport. Management Systems In Production Engineering, 29(2), 91-96

Konstanty, J., Radek, N., Scendo, M., 2015. The electro-spark deposited WC-Cu coatings modified by laser treatment, Archives of Metallurgy and Materials. 60(4), 2579-2584, DOI: 10.1515/amm-2015-0417

Kraus, V., 1980. Vypocet teplot radiacich lamelovych spojok a brzd (Calculation of temperature multi-disc shifting brake and shifting clutches). Habitation thesis. Žilina: Edis ZU. Slovak.

Kucera, L., Gajdosik, T., Gajdac, I., Miskolci, J., 2021. Alternatívne pohony (Alternative drives). EDIS ZU, Zilina, Slovakia.

Liptakova, T., Broncek, J., Lovisek, M., Lago, J., 2017. Tribological and corrosion properties of Al-brass. 33rd Danubia Adria Symposium on Advances in Experimental Mechanics, Portorož, Slovenia, 5867-5871.

Mruzek, M., Gajdac, I., Kucera, L., Barta, D., 2015. Analysis of Parameters Influencing Electric Vehicle Range. Transbaltica 2015: 9th International Scientific Conference, Vilnius, Lithuania, 165-174.

Mruzek, M., Gajdac, I., Kucera, L., Gajdosik, T., 2017.The Possibilities of Increasing the Electric Vehicle Range. 12th international scientific conference of young scientists on sustainable, modern and safe transport, High Tatras, Slovakia, 621-625.

Narula, S., Puppala, H., Kumar, A., Frederico, G., F., Dwivedy, M., Prakash, S., Talwar, V., 2021. Applicability of industry 4.0 technologies in the adoption of global reporting initiative standards for achieving sustainability. Journal of Cleaner Production, 305, 127141, DOI: 10.1016/j.jclepro.2021.127141

Porsche, 2022, Technical article: Porsche Surface Coated Brakes Hard like diamond. available at: https://dealer.porsche.com/my/sungaibesi/en-

GB/Offers/Technical-article-porsche-surface-coated-brakes-519 (accessed 4 October 2022)
Qiu, C., Wang, G., Meng, M., Shen, Y., 2018. A novel control strategy of regenerative braking system for electric ve-hicles under safety critical driving situations, Energy. 149, 329-340, DOI: 10.1016/j.energy.2018.02.046
QS-Motor, 2022. 4WD 8000W 96V E-Car Hub Motor Conversion kits. available at: http://www.qs-motor.com/product/qsmotor-4wd-8000w-96v-electric-car-hub-motor-conversion-kits/ (accessed 5 October 2022)
QS-Motor, 2022. QS273 8000W 50H V3 Electric Car Hub Motor. available at: http://www.qs-motor.com/product/3000w-8000w-electric-car-hub-motor273-model/ (accessed 5 October 2022)
Radek, N., Antoszewski, B., 2009. Influence of laser treatment on the properties of electrospark deposited coatings. Mettalic Materials, 47(1), 31-38.
Radek, N., Bartkowiak, K., 2010. Performance properties of electro-spark deposited carbide – ceramic coating modified by laser beam. LANE 2010, Erlangen-Nuremberg, Germany, 417-423.
Radek, N., Pietraszek, J., Gadek-Moszczak, A., Orman, L., J., Szczotk, A., 2020. Themorphology and mechanical properties of ESD coatings before and after Laser Beam Machining. Materials, 13(10), 2331, DOI: 10.3390/ma13102331
Radek, N., Szczotok, A., Gądek-Moszczak, A., Dwornicka, R., Broncek, J., Pietraszek, J., 2018. The impact of Laser processing parameters on the properties of electro spark deposited coatings. Archives of Metallurgy and Materials, 63(2), 809-816, DOI: https://doi.org/10.24425/122407
Rovňák , M., Kalistová, A, Štofejová, L., Benko, M., Salabura, D., 2022. Management Of Sustainable Mobility and The Perception of The Concept of Electric Vehicle Deployment. Polish Journal Of Management Studies; 25 (2), 266-281, Doi: 10.17512/Pjms.2022.25.2.17
Siedlecka, U., 2019. Heat Conduction in the Finite Medium Using the Fractional Single-Phase-Lag Model. Bulletin of the Polish Academy of Sciences: Technical Sciences, 67 (2), 401-407, DOI: 10.24425/bpas.2019.128599
Spałek, D., 2018. Two Relations for Generalized Discrete Fourier Transform Coefficients. Bulletin of the Polish Academy of Sciences: Technical Sciences, 66(3), 275-281, DOI: 10.24425/123433
Staniszewska, E., Klimecka-Tatar, D., Obrecht, M., 2020. .Eco-design processes in the automotive industry. Production Engineering Archives. 26(4) 131-137, DOI: 10.30657/pea.2020.26.25
Strojirenstvi, 2020. Špeciálne elektrické vozidlo z nekonvenčných materiálov do ťažkých podmienok (A special electric vehicle made of unconventional materials for difficult conditions), available: https://www.strojirenstvi.cz/specialne-elektricke-vozidlo-z-nekonvencnych-materialov-do-tazkych-podmienok (accessed 10 October 2022)
Strojirenstvi, 2021. Optimalizácia zavesenia nápravy vozidla MODULO s pomocou ad-itívnych technológií. (Optimizing the axle suspension of the MODULO vehicle with the help of additive technologies), available: https://www.strojirenstvi.cz/optimalizacia-zavesenia-napravy-vozidla-modulo-s-pomocou-aditivnych-technologii (accessed 9 October 2022)
Synopsys, 2022. What is ISO 26262? available at: https://www.synopsys.com/automotive/what-is-iso-26262.html (accessed 5 October 2022)
Tejado, E., Dias, M., Correia, J., Palacios, T., Carvalho, P., Alves, E., Pastor, J., Y., 2018. New WC-Cu thermal barriers for fusion applications. High temperature mechanical behaviour, Journal of Nuclear Materials, 498, 355-361, DOI: 10.1016/j.jnucmat.2017.10.071
Tomasikova, M., Tropp, M., Gajdosik, T., Krzywonos, L., Brumercik, F., 2017. Analysis of Transport Mechatronic System Properties. 12th international scientific conference of young scientists on sustainable, modern and safe transport, High Tatras, Slovakia, 881-886.
Tropp, M., Tomasikova, M., Bastovansky, R., Krzywonos, L., Brumercik, F., 2017. Concept of Deep Drawing Mechatronic System Working in Extreme Conditions. 12th international scientific conference of young scientists on sustaina-ble, modern and safe transport, High Tatras, Slovakia, 893-898.
Tropp, M., Tomasikova, M., Bastovansky, R., Krzywonos, L., Brumercik, F., 2017. Transient thermal simulation of working components of mechatronic system for deep drawing of molybdenum sheets. 58th International Conference of Machine Design Departments, Prague, Czech Republic, 408-413.
University of Zilina, 2018. International Exhibition of Technical Innovations, Patents and Inventions – 3 awards for FME. available at: https://www.fstroj.uniza.sk/index.php/en/oznamy-pre-zamestnancov/1754-technical-innovations-patents-and-inventions. (accessed 5 October 2022)
Varecha, D., Broncek, J., Kohar, R., Novy, F., Vicen, M., Radek, N., 2021. Research of friction materials applicable to the multi-disc brake concept. Journal of Materials Research and Technology, 14, 647-661, DOI: 10.1016/j.jmrt.2021.06.061
Varecha, D., Kohar, R., Brumercik, F., 2019. AGV brake system simulation. Logi: Scientific Journal on Transport and Logistics, 10 (1), 1-9, DOI: 10.2478/logi-2019-0001.
Varecha, D., Kohar, R., Gajdosik, T., 2019. Optimizing the braking system for handling equipment. 9th International Scientific Conference – Research and Development of Mechanical Elements and Systems, Kragujevac, Serbia 1-10.
Varecha, D., Kohar, R., Lukac, M., 2021. Theoretical study of heat conduction in the multi-disc brake integrated into the drive wheel AGV during braking. Bulletin of the Polish Academy of Sciences: Technical Sciences, 69(2), e136718, DOI: https://doi.org/10.24425/bpasts.2021.136718
Volkswagen UK, 2022. Electric Car Regenerative Braking - Brake energy recuperation. available at: https://www.volkswagen.co.uk/en/electric-and-hybrid/sustainability/brake-energy-recuperation.html (accessed 5 October 2022)
Wolf, K., B., 1979. Integral transforms in science and engineering. 1st Edition, Springer New York, NY.
Zhao, J., Yu, DQ, L., 2004. Improvement on the microstructure stability. Mechanical and Wetting Properties of Sn-Ag-Cu Lead-Free Solder with the Addition of rare earth elements, Journal of Alloys and Compounds, 376(1-2), 170-175, DOI: 10.1016/j.jallcom.2004.01.012

Appendix

Appendix A

Equations 9 Fourier partial differential equation for non-stationary heat conduction for temperature profile calculation

$$\frac{\vartheta_{(x,t)}}{\vartheta_o} = \frac{2.t^*}{t_b}.\left(1-\frac{t^*}{2.t_b}\right)+\frac{4}{\pi^2}.G.\sum_{m=1}\frac{\cos\left(m.\pi.\frac{x}{h}\right)}{m^2}.\left[\left(1+\frac{G}{m^2.\pi}-\frac{t^*}{t_b}\right).e^{-\frac{m^2.\pi^2}{G}\left(\frac{t}{t_b}-\frac{t^*}{t_b}\right)}-\left(1+\frac{G}{m^2.\pi}\right).e^{-\frac{m^2.\pi^2}{G}.\frac{t}{t_b}}\right]$$

实验模块电动汽车WC-Cu刹车系统摩擦学和热力学参数研究

關鍵詞
WC-Cu涂层
摩擦系数
电动车
刹车系统
制动模拟

摘要
本文作者介绍了一种基于WC-Cu摩擦材料的电动汽车刹车系统的发展。本文是AGV多盘刹车系统的原始发展和WC-Cu涂层摩擦系数的实验研究的延续。除了开发电动汽车的机械元素和结构外，还在摩擦实验室研究了钢基体C45与WC-Cu涂层的三个样品的摩擦学参数。使用电火花沉积涂层技术在C45钢基体上施加WC-Cu基础金属涂层。实验使用了三个样品，其中包含涂层结构中化学元素的不同百分比比例。在实验期间，使用“球板”原理的摩擦计研究了所有样品的摩擦系数。随后，使用激光技术修改了样品的表面结构WC-Cu。接下来阶段使用维氏方法调查了修饰和未修饰涂层的硬度。在实验研究结束时在Matlab®软件的编程环境中创建了一个刹车模拟，考虑了所有驱动阻力。研究人员还关注了在刹车时的热传导模拟，考虑了一些在水平和20%坡道上刹车的驾驶模式。使用离散傅里叶偏微分方程